2. Dating Methods and Corresponding Chronometers in Astrobiology

MURIEL GARGAUD
Observatoire Aquitain des Sciences de l'Univers, Université Bordeaux 1, Bordeaux, France
(E-mail: gargaud@obs.u-bordeaux1.fr)

FRANCIS ALBARÈDE
Ecole Normale Supérieure, Lyon, France
(E-mail: albarede@ens-lyon.fr)

LAURENT BOITEAU
Départment de Chimie, Université Montpellier II, Montpellier, France
(E-mail: laurent.bioteau@unive-montp2.fr)

MARC CHAUSSIDON
Centre de Recherches Pétrographiques et Géochimiques (CRPG), Nancy, France
(E-mail: chocho@crpg.cnrs-nancy.fr)

EMMANUEL DOUZERY
Institut des Sciences de l'Evolution, Université Montpellier II, Montpellier, France
(E-mail: douzery@isem.univ-montp2.fr)

THIERRY MONTMERLE
Laboratoire d'Astrophysique de Grenoble, Université Joseph Fourier, Grenoble, France
(E-mail: montmerle@obs.ujf-grenoble.fr)

Abstract. This chapter concerns the tools with which time or durations are measured in the various disciplines contributing to the chronology of the solar system until the emergence of life. These disciplines and their tools are successively: astronomy (use of the Herzsprung–Russell diagram), geochemistry (radioactive dating), chemistry (no clocks!), and biology (molecular clocks, based on rates of molecular evolution over phylogenetic trees). A final section puts these tools in perspective, showing the impossibility of using a unique clock to describe the evolution of the solar system and of life until today.

Keywords: Dating methods, chronometers, Herzsprung-Russel diagram, radioactive dating, molecular clocks

2.1. Astronomy: Dating Stellar Ages with the "Herzsprung–Russell Diagram"

THIERRY MONTMERLE

Since the beginning of the 20th century, astronomers have been using the "Herzsprung–Russell Diagram" (after the name of its discoverers; "HRD" for short) to classify stars and understand their evolution.

Observationally, astronomers first determine the magnitude and spectral type of the stars. These numbers are then transformed into luminosity L_* and temperature T_{eff}, which are physical quantities that can be compared with models. This assumes (i) knowing the distance (to convert magnitudes into luminosities), which is determined by various methods (to an accuracy of ~20–30% in the case of young stars), and (ii) converting from spectral types to temperatures, which can be done with models of stellar photospheres. For "simple" stars like the Sun, the temperature determination is very precise (<1%), but for more complex spectra, like Young stars (T Tauri stars) which have a circumstellar disk, the uncertainty may reach 10–20% or more.

In the course of their evolution, stars live two fundamentally different lives. As is now well understood, stars like the Sun are in a quiet stage, lasting billions of years, in which hydrogen is slowly converted into helium: this is known as the "main sequence". The evolution continues after the main sequence in a more complex way, but the energy output is always *thermonuclear* in origin, with successive nuclear reaction networks driving important changes in the overall stellar structure (like the formidable expansion phase of solar-type stars, known as "red giants", in which the stellar radius becomes larger than the size of the solar system, ending in spectacular "planetary nebulae"). This evolution is strongly dependent on mass: the most massive stars (>10 $M_{\odot}$[1] end their lives in catastrophic explosive events known as supernovae that entirely disrupt them. At the other end of the mass spectrum, low-mass stars (<0.7 $M_{\odot}$) are essentially eternal: their lifetimes are longer than the age of the universe!

Figure 2.1.1 summarizes two important factors that crucially depend on stellar mass (adapted from Montmerle and Prantzos, 1988): the stellar luminosity (left) and the stellar lifetime (right). One can see that stellar luminosities (*on the main sequence*) span 9 orders of magnitude (L_* from 10^{-3} $L_{\odot}$[2] to 10^6 $L_{\odot}$), for masses M_* between 0.1 and 100 $M_{\odot}$. This is an expression of the well-known law $L_* \propto M_*^3$, which can be demonstrated when the stellar energy is derived only from the conversion of hydrogen into helium. Correspondingly, massive stars burn more hydrogen per unit time than lower-mass stars, and above 20 $M_{\odot}$ live only a few million years.

Figure 2.1.2 (also adapted from Montmerle and Prantzos, 1988) summarizes the fate of stars, depending on their mass. In brief, low-mass stars, including the Sun ($M_* < 6$–7 $M_{\odot}$), become "red giants" and lose mass to expand as "planetary nebulae" after 10^8–10^9 yrs, leaving behind an Earth-sized, very hot (10^5 K) compact star: a "white dwarf". More massive stars evolve faster (Figure 2.1.1) and end their lives exploding as supernovae,

---

[1] $M_{\odot}$ = 1 Solar mass = 1.989×10^{30} kg

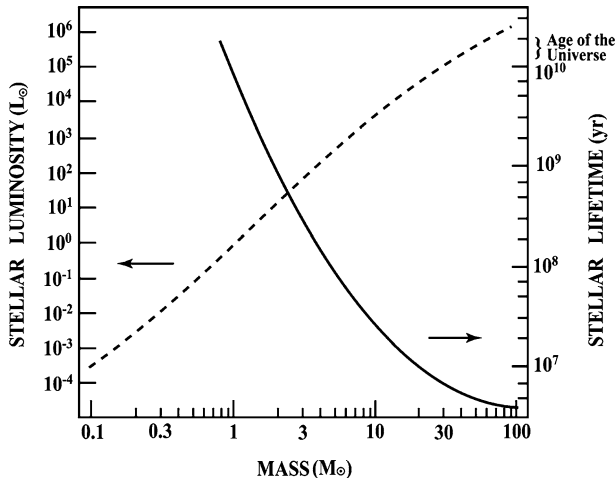[2] $L_{\odot}$ = 1 Solar luminosity = 3.826×10^{26} w

Figure 2.1.1. Stellar luminosity on the main sequence (dotted line, left-hand scale) and stellar lifetimes (continuous line, right-hand scale), as a function of mass. The most massive stars radiate an enormous power (up to 1 million suns), but have extremely brief lifetimes (a few million years), whereas low-mass stars ($M_* < 0.7 M_{\odot}$) are extremely faint (less than 10^{-4} suns) and are essentially "eternal", i.e., have lifetimes longer than the age of the universe (currently accepted value: 13.7 billion years).

themselves leaving behind even more compact, city-sized stars (neutron stars, black holes). Since the most massive stars live only a few million years, they explode as supernovae in the same region as where they were born, and interact violently with their parent molecular cloud, possibly triggering new generations of stars, and "polluting" the cloud with freshly synthesized elements such as the short-lived radioactive nuclei ^{26}Al and ^{60}Fe (see Section 3.2.2.3).

Before the main sequence, however, the situation is entirely different, since the stars slowly shrink as the radiation generated by gravitational contraction is evacuated in the form of light. In other words, the energy of "pre-main sequence" stars (protostars and T Tauri stars) in *not nuclear* in origin, but is drawn only from *gravitation*. This "simplification" explains that, as early as 1966 (when only low-power computers were available!), the first theoretical model of pre-main sequence evolution could be devised by Hayashi and his collaborators in Japan (Hayashi, 1966).

This early work on "Hayashi" evolutionary tracks in the HRD (luminosity as a function of temperature) distinguished two main phases which are still used as a reference today:

(i) The "convective" phase, in which the stars are fully convective, and evolve essentially isothermally (i.e., at the same temperature, so that the theoretical tracks as a function of mass are all approximately vertical);
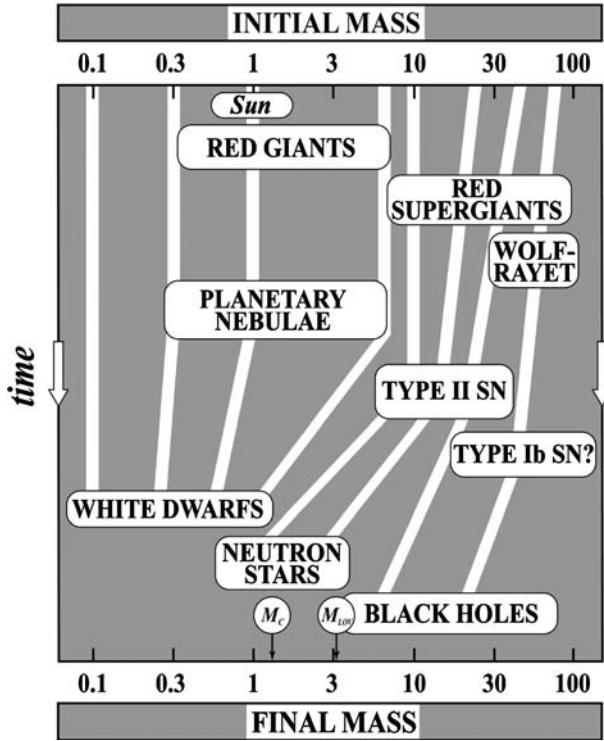
Figure 2.1.2. Stellar evolution in a nutshell: the fate of stars as a function of their initial mass (in $M_\odot$). The mass stays constant on the main sequence (vertical line as a function of time), but as a result of nuclear reactions and changes of structure, all stars start to lose mass, at a rate which increases with the mass (evolutionary line bent to the left). They all end in "compact objects", when reaching a final, critical mass in their core: Earth-sized "white dwarfs", up to ~1 $M_\odot$, the "Chandrasekhar mass" ($M_C = 1.4 \ M_\odot$) for neutron stars, and the "Landau–Oppenheimer–Volkoff" mass ($M_{LOV} = 3.1 \ M_\odot$) for black holes.

(ii) The "radiative" phase, in which a radiative core develops inside the star, which then becomes hotter but evolves at an almost constant luminosity (following the contraction in radius).

For a star like the Sun, the convective phase lasts about 10 million years, during which the temperature is held almost constant, around 4600 K, and the luminosity drops by a factor of ~20 with respect to the early T Tauri stage (when the young Sun starts to be optically visible). Then the radiative phase lasts from ~10 million to ~100 million years at a roughly constant luminosity (~1 L_{sun}), until the central regions become hot enough (15 MK) that thermonuclear reactions transforming hydrogen into helium start. This marks the beginning of the main sequence, on which the Sun has been for ~4.5 billion
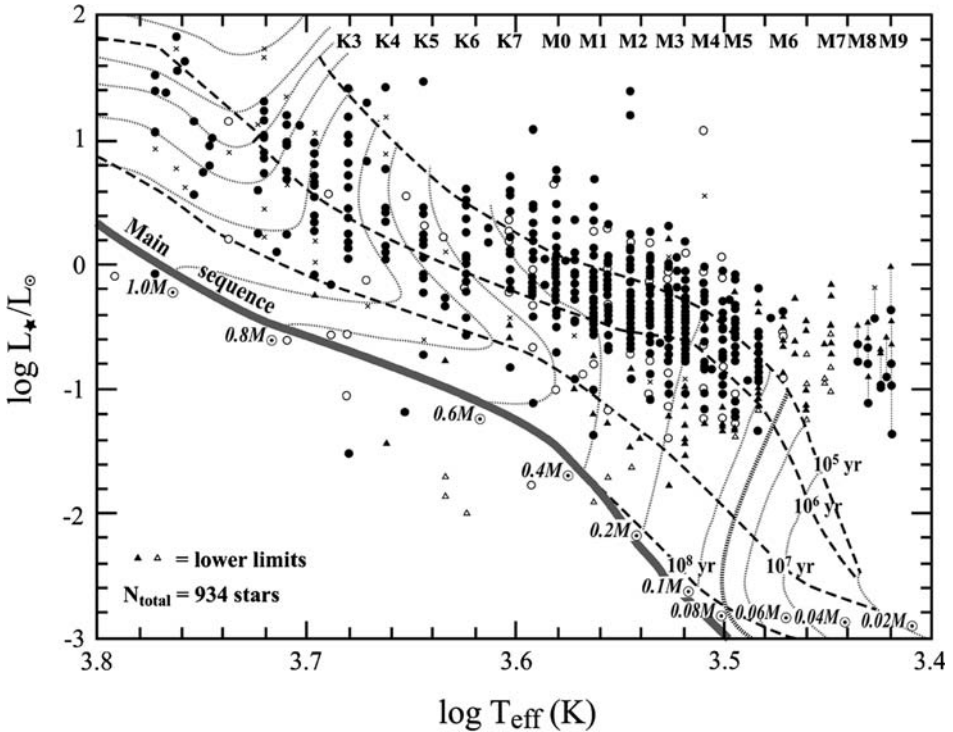
Figure 2.1.3. Herzsprung–Russell diagram of 934 low-mass members of the Orion Nebula Cluster (adapted from Hillenbrand, 1997). The spectral types corresponding to surface temperatures (T_{eff}) are also indicated at the top of the diagram. The theoretical grid is labeled in masses, from 0.02 to 5 $M_{\odot}$ (dotted lines; the upper left-hand dotted lines for higher masses are highly uncertain) and ages, from 10^5 to 10^8 yrs (dashed lines). The main sequence is also indicated. The thick dotted line to the right indicates the theoretical evolution of stars of mass < 0.08 $M_{\odot}$ (brown dwarfs), which never ignite nuclear reactions, hence never reach the main sequence.

years and will be for the next ~5 billion years, before it becomes, as mentioned above, a solar-system-sized red giant and then a planetary nebula.

The pre-main sequence phase is illustrated more generally in Figure 2.1.3 by the HRD of the Orion Nebula Cluster ("ONC"), the classic cluster associated with the Orion nebula M42, adapted from Hillenbrand (1997). The reason for this choice is far from arbitrary: we now believe (see Chapter 3) that the Sun was probably formed in a similar star cluster. The ONC itself comprises about 2000 stars, of which the best characterized 934 low-mass stars are plotted in the diagram (dots). The observational points lie in a grid of theoretical lines: (i) the dotted lines label stellar masses, from 0.02 $M_{\odot}$, to 5 $M_{\odot}$, with a thick dotted line marking the mass boundary below which stars never ignite thermonuclear reactions (the so-called "brown dwarfs"); (ii) the oblique dashed lines correspond to stellar ages, labelled by factors of 10, from

10^5 yr (top) to 10^8 yr (bottom, main sequence). As they evolve, the stars follow the "Hayashi evolutionary tracks" (dotted lines), successively convective and radiative as explained above for the Sun (1 $M_\odot$ by definition), until they reach the main sequence.

Then in such a diagram each (L_*, T_{eff}) observational point is converted, via theoretical model grids, into (mass, age) estimates (see Hillenbrand, 1997 for details and references; new theoretical models have been constructed since that paper, especially covering the high-mass and very low-mass ends: e.g., Chabrier and Baraffe, 2000; Palla and Stahler, 2001). For the ONC, one sees that the observed masses for the majority of stars run from ~0.1 $M_\odot$ to 5 $M_\odot$ and above, and the ages from less than (i.e., younger than) 10^5 yrs to a few million years. Ages smaller than 10^5 yrs are very uncertain, and all the stars shown should be understood as being "very young" only. The age of older stars (>10^6 yrs) is more reliable (uncertainty ~20–30%). One major conclusion from this diagram is that star formation in Orion has not been instantaneous, but is spread over a few million years and still continues today (see Section 3.2.2.3).

2.2. Geochemistry: Principles of Radioactive Dating

FRANCIS ALBARÈDE AND MARC CHAUSSIDON

A number of radioactive elements were present in the solar system when it formed. As a consequence, geochemical ages can be obtained for a given rock from the amount of daughter isotopes that have been accumulated in its different minerals via radioactive decay of the parent isotopes. It must be noted that the proportions of parent isotopes remaining in rocks have no relationship with the age of the rock, but are a direct function of the age of the considered chemical element, i.e., the average time elapsed since the nucleosynthesis of this element. The strength of isotopic dating is that radioactive decay is a nuclear process so that the rate of decay is constant and thus independent of the history of a rock.

Radioactivity is a memoryless process (atoms do not age) and is therefore a nuclear event whose probability of occurrence per unit of time, noted λ, is independent of time. This probability, termed the *decay constant*, is specific to each radioactive nuclide. Radioactive decay is a Poisson process, where the number of events is proportional to the time over which the observation is made. In the absence of any other loss or gain, the proportion of parent atoms (or radioactive nuclides) disappearing per unit of time t is constant:

$$\frac{dP}{Pdt} = -\lambda. \tag{1}$$

Occasionally, the notions of half-life or of mean life are used instead of λ. The half-life $(T_{1/2})$ is the time required for the decay of half the number of radioactive atoms originally present in the system:

$$T_{1/2} = \frac{\ln 2}{\lambda}. \tag{2}$$

The mean life (τ) is the inverse of the decay constant $(\tau = 1/\lambda)$, it differs from the half-life $T_{1/2}$ by a factor $\ln 2$. The values of λ and $T_{1/2}$ of the main radiometric chronometers are given in Table 2.1.

For a number of parent atoms $P = P_0$ at time $t = 0$, Equation (1) integrates as:

$$P = P_0 e^{-\lambda t}. \tag{3}$$

It is therefore possible to determine the age of a system by measuring the number P of parent atoms that it contains today. However, this requires P_0 to be known and therefore, in this form, Equation (3) is in general not a chronometer (a notable exception is the ^{14}C method). For each parent atom, a daughter atom (or radiogenic nuclide) is created, usually of a single element, whose amount can be noted D. In a closed system and for a stable daughter nuclide D, the number of parent and daughter atoms is constant, therefore:

$$D = D_0 + P_0 - P = D_0 + P(e^{\lambda t} - 1). \tag{4}$$

The term $P(e^{\lambda t} - 1)$ is a measure of the radiogenic nuclides accumulated during time t, D_0 being the amount of isotope D at $t = 0$, therefore:

$$t = \frac{1}{\lambda} \ln\left(1 + \frac{D - D_0}{P}\right). \tag{5}$$

Even if D and P are measured, this equation is no more a timing device than Equation (3), unless the number of daughter atoms D_0 at time $t = 0$ is known.

Two different types of radioactive isotopes can be used to constrain the timescales of the formation of the solar system:

• Radioactive elements with a long half-life are useful to determine absolute ages for the different components of meteorites. The most commonly used long-lived nuclides are ^{235}U $(T_{1/2} = 0.704$ Ga), ^{238}U $(T_{1/2} = 4.47$ Ga), ^{87}Rb $(T_{1/2} = 48.81$ Ga), ^{147}Sm $(T_{1/2} = 106$ Ga) and ^{176}Lu $(T_{1/2} = 35.9$ Ga); see Table 2.1 for details.

MURIEL GARGAUD ET AL.

TABLE 2.1
Decay constant λ and half life ($T_{(1/2)}$) for main radiometric chronometer

Parent nuclide	Daughter nuclide	λ = Decay constant	$T_{1/2}$ = Half life
^{7}Be	^{7}Li	4,7735 yr^{-1}	53 d
^{228}Th	^{224}Ra	3.63×10^{-1} yr^{-1}	1.91 yr
^{210}Pb	^{210}Bi	3.11×10^{-2} yr^{-1}	22.3 yr
^{32}Si	^{32}P	2.1×10^{-3} yr^{-1}	330 yr
^{226}Ra	^{222}Rn	4.33×10^{-4} yr^{-1}	1.60×10^3 yr
^{14}C	^{14}N	1.245×10^{-4} yr^{-1}	5.59×10^3 yr
^{231}Pa	^{227}Ac	2.11×10^{-5} yr^{-1}	3.29×10^4 yr
^{230}Th	^{226}Ra	9.21×10^{-6} yr^{-1}	7.53×10^4 yr
^{59}Ni	^{59}Co	9.12×10^{-6} yr^{-1}	7.60×10^4 yr
^{41}Ca	^{41}K	6.93×10^{-6} yr^{-1}	1.00×10^5 yr
^{81}Kr	^{81}Br	3.03×10^{-6} yr^{-1}	2.29×10^5 yr
^{234}U	^{230}Th	2.83×10^{-6} yr^{-1}	2.45×10^5 yr
^{36}Cl	^{36}Ar	2.30×10^{-6} yr^{-1}	3.01×10^5 yr
^{26}Al	^{26}Mg	9.80×10^{-7} yr^{-1}	7.07×10^5 yr
^{107}Pd	^{107}Ag	6.5×10^{-7} yr^{-1}	1.07×10^6 yr
^{60}Fe	^{60}Ni	4.62×10^{-7} yr^{-1}	1.50×10^6 yr
^{10}Be	^{10}B	4.59×10^{-7} yr^{-1}	1.51×10^6 yr
^{53}Mn	^{53}Cr	1.87×10^{-7} yr^{-1}	3.71×10^6 yr
^{182}Hf	^{182}W	7.7×10^{-8} yr^{-1}	9.00×10^6 yr
^{129}I	^{129}Xe	4.3×10^{-8} yr^{-1}	1.61×10^7 yr
^{92}Nb	^{92}Zr	1.93×10^{-8} yr^{-1}	3.59×10^7 yr
^{244}Pu	$^{131-136}$Xe	8.66×10^{-9} yr^{-1}	8.00×10^7 yr
^{235}U	^{207}Pb	9.849×10^{-10} yr^{-1}	7.04×10^8 yr
^{146}Sm	^{142}Nd	6.73×10^{-10} yr^{-1}	1.03×10^9 yr
^{40}K	^{40}Ar	5.50×10^{-10} yr^{-1}	1.26×10^9 yr
^{40}K	^{40}Ca	4.96×10^{-10} yr^{-1}	1.40×10^9 yr
^{187}Re	^{187}Os	1.64×10^{-11} yr^{-1}	4.23×10^{10} yr
^{238}U	^{206}Pb	1.551×10^{-10} yr^{-1}	4.47×10^9 yr
^{87}Rb	^{87}Sr	1.42×10^{-11} yr^{-1}	4.88×10^{10} yr
^{40}K	^{40}Ar	5.81×10^{-11} yr^{-1}	1.19×10^{10} yr
^{232}Th	^{208}Pb	4.95×10^{-11} yr^{-1}	1.40×10^{10} yr
^{176}Lu	^{176}Hf	1.93×10^{-11} yr^{-1}	3.59×10^{10} yr
^{147}Sm	^{143}Nd	6.54×10^{-12} yr^{-1}	1.06×10^{11} yr
^{138}La	^{138}Ce	2.24×10^{-12} yr^{-1}	3.09×10^{11} yr
^{130}Te	^{130}Xe	8.66×10^{-23} yr^{-1}	8.00×10^{21} yr

- Radioactive elements with a short half-life are useful to build a relative chronology with a sharp time resolution (on the order of the half-life or shorter) for early solar system processes. These short-lived radioactive elements are also called *extinct radioactivities* or *extinct radioactive nuclides*, as per today, 4.56 Ga after the formation of the solar system, they have totally decayed and are no more present in meteorites, yet their former presence can be inferred by the presence of their daughter products. It is for this type of radioactive elements that a so-called "last minute origin" (see Chapter 3) is required to explain their presence in the early Solar system. The short-lived nuclides detected so far are ^{7}Be ($T_{1/2} = 53$ days), ^{41}Ca ($T_{1/2} = 0.1$ Ma), ^{36}Cl ($T_{1/2} = 0.301$ Ma), ^{26}Al ($T_{1/2} = 0.707$ Ma), ^{10}Be ($T_{1/2} = 1.51$ Ma), ^{60}Fe ($T_{1/2} = 1.5$ Ma) and ^{53}Mn ($T_{1/2} = 3.71$ Ma); see Table 2.1 for details.

2.2.1. LONG-LIVED CHRONOMETERS

2.2.1.1. *"Rich" chronometers: $D_0 \ll D$*
The condition $D_0 \ll D$ applies for instance to the U–Pb dating of zircons, in which the amounts of initial ^{206}Pb and ^{207}Pb are negligible when compared to ^{206}Pb and ^{207}Pb produced by the radioactivity of ^{238}U and ^{235}U, respectively (radiogenic ingrowth). Equation (5) may then be written:

$$t = \frac{1}{\lambda_{^{238}U}} \ln\left(1 + \frac{^{206}Pb_t}{^{238}U_t}\right)$$

This condition is also met for the K–Ar dating method.

These ages date the isolation of the analysed mineral, and consequently, they can be different from the age of the host rock.

2.2.1.2. *"Poor" chronometers: the isochron method*
When the condition $D_0 \ll D$ does not apply, it is replaced by the principle of isotopic homogenisation. When mineral phases, melts and fluids, separate from each other, such as during melting, vaporisation, or metamorphic alteration, it is safely assumed that these processes do not selectively separate the radiogenic from stable nuclides (other isotope fractionation processes, either natural or instrumental, are corrected using a different pair of stable isotopes from the same element). Equation (4) is transformed by dividing each member by the number D' of atoms of a stable isotope (i.e., neither radioactive nor radiogenic) of D. For a closed system, D' remains constant and therefore:

$$\left(\frac{D}{D'}\right)_t = \left(\frac{D}{D'}\right)_0 + \left(\frac{P}{D'}\right)_t (e^{\lambda t} - 1). \tag{6}$$

For the ^{87}Rb–^{87}Sr chronometer $P = {}^{87}$Rb, $D = {}^{87}$Sr, and $D' = {}^{86}$Sr, and therefore:

$$\left(\frac{^{87}\text{Sr}}{^{86}\text{Sr}}\right)_t = \left(\frac{^{87}\text{Sr}}{^{86}\text{Sr}}\right)_0 + \left(\frac{^{87}\text{Rb}}{^{86}\text{Sr}}\right)_t \left(e^{\lambda_{87}\text{Rb}\,t} - 1\right).$$

In this equation, D/D' represents the ratio of the radiogenic nuclide to its stable isotope (e.g., ^{87}Sr/^{86}Sr) and P/D' is the "parent/daughter" ratio, called this way as in practice it is proportional to an elemental ratio (here Rb/Sr). In a diagram (^{87}Sr/^{86}Sr) versus (^{87}Rb/^{86}Sr), several samples formed at the same time from a well-mixed reservoir (meteorites from the nebula, rocks from a magma) define a straight-line called "isochron" and the slope a of this line, which simply is $e^{\lambda_{87}\text{Rb}\,t} - 1$, gives the age t of the rock as:

$$t = \frac{1}{\lambda_{87}\text{Rb}} \ln a.$$

This isochron equation can be graphically solved if, in the sample to be dated, several fractions having different parent/daughter ratios (^{87}Rb/^{86}Sr) can be analysed (Figure 2.2.1).

This age dates the time at which the two samples last shared a same ^{87}Sr/^{86}Sr ratio. This method is commonly used for parent–daughter systems with a long half-life, typically ^{143}Nd–^{144}Nd, ^{176}Lu–^{176}Hf and ^{187}Re–^{187}Os.

A particular application combines the two chronometers ^{238}U–^{206}Pb and ^{235}U–^{207}Pb, in which the parent isotopes (^{238}U and ^{235}U) are not explicitly considered but only the daughter isotopes (^{206}Pb–^{207}Pb); this method is known as the Pb–Pb method.

2.2.2. Short-lived chronometers: extinct radioactivities

The so-called extinct radioactivities (see Section 3.2.2) have a short half-life ($T_{1/2}$) and therefore a large λ. For large values of λt, P becomes vanishingly small and therefore the closed system condition reads:

$$D_{\text{today}} = (D + P)_t \tag{7}$$

for any sample formed at any time t after the isolation or the solar system from the nucleosynthetic processes. Let us write this equation for a sample (spl) formed from the solar nebula (SN), which we suppose to be isotopically homogenous, and divide it by D':

$$\left(\frac{D}{D'}\right)_{\text{today}}^{\text{spl}} = \left(\frac{D}{D'}\right)_t^{\text{spl=SN}} + \left(\frac{P}{P'}\right)_t^{\text{spl=SN}} \left(\frac{P'}{D'}\right)_{\text{today}}^{\text{spl}} \tag{8}$$
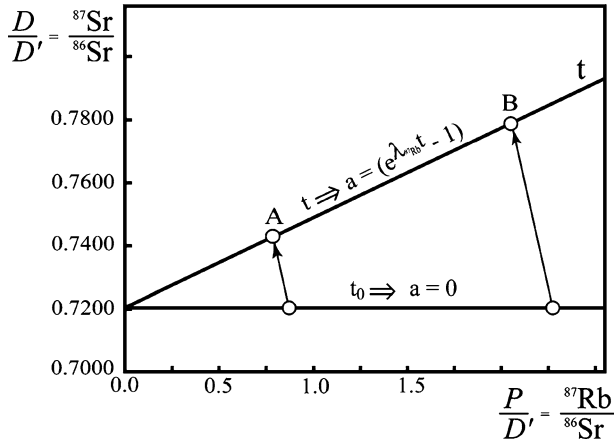
Figure 2.2.1. D/D' vs. P/D' isochron diagram showing how the slope a of the "isochron" is a time dependent parameter, whose knowledge allows to calculate time t. See other examples in Chapter 3.2: Figures 3.2.7, 3.2.8.

in which, as above, P' is an isotope of the parent nuclide P, and the closed system assumption $(P')_t = (P')_0$ holds. This equation is equivalent to:

$$\left(\frac{D}{D'}\right)^{\text{spl}}_{\text{today}} = \left(\frac{D}{D'}\right)^{\text{SN}}_{\text{today}} + \left(\frac{P}{P'}\right)^{\text{sple=SN}}_{t}\left[\left(\frac{P'}{D'}\right)^{\text{spl}}_{\text{today}} - \left(\frac{P'}{D'}\right)^{\text{SN}}_{\text{today}}\right] \tag{9}$$

in which we used a transformation of Equation (7) as:

$$\left(\frac{D}{D'}\right)^{\text{SN}}_{t} = \left(\frac{D}{D'}\right)^{\text{SN}}_{\text{today}} - \left(\frac{P}{D'}\right)^{\text{SN}}_{t} = \left(\frac{D}{D'}\right)^{\text{SN}}_{\text{today}} - \left(\frac{P}{P'}\right)^{\text{SN}}_{t}\left(\frac{P'}{D'}\right)^{\text{SN}}_{\text{today}} \tag{10}$$

with the usual closed-system constraint on both D' and P'.

In the case of the ^{26}Al–^{26}Mg chronometer, Equation (8) reads:

$$\left(\frac{^{26}\text{Mg}}{^{24}\text{Mg}}\right)^{\text{spl}}_{\text{today}} = \left(\frac{^{26}\text{Mg}}{^{24}\text{Mg}}\right)^{\text{spl=SN}}_{t} + \left(\frac{^{26}\text{Al}}{^{27}\text{Al}}\right)^{\text{spl=SN}}_{t}\left(\frac{^{27}\text{Al}}{^{24}\text{Mg}}\right)^{\text{spl}}_{\text{today}}$$

which, for a set of samples formed at time t from a homogeneous nebula, is the equation of an isochron in a ^{26}Mg/^{24}Mg vs. ^{27}Al/^{24}Mg plot. Both the slope and the intercept of the isochron (which revolves around the point representing the solar nebula) are time-dependent.

The ^{26}Al/^{27}Al ratio of the solar nebula at the time a particular sample formed is obtained by isolating the $(P/P')_t$ ratio from equation (9), here for ^{26}Al:

$$\left(\frac{^{26}\text{Al}}{^{27}\text{Al}}\right)_t^{\text{spl}=\text{SN}} = \left(\frac{^{26}\text{Al}}{^{27}\text{Al}}\right)_0^{\text{SN}} e^{-\lambda t} = \frac{(^{26}\text{Mg}/^{24}\text{Mg})_{\text{today}}^{\text{spl}} - (^{26}\text{Mg}/^{24}\text{Mg})_{\text{today}}^{\text{SN}}}{(^{27}\text{Al}/^{24}\text{Mg})_{\text{today}}^{\text{spl}} - (^{27}\text{Al}/^{24}\text{Mg})_{\text{today}}^{\text{SN}}}.$$

If the $^{26}\text{Al}/^{27}\text{Al}$ ratio of the solar nebula at the reference time $t = 0$ is assumed, the result can be converted into an age. This age dates the time at which the sample shared the same $^{26}\text{Al}/^{27}\text{Al}$ ratio as the solar nebula. If no history of the $^{26}\text{Al}/^{27}\text{Al}$ ratio is assumed for the solar nebula, dividing this equation for one sample by the same equation for a second sample gives the age difference between the two samples. This method is used for a number of "extinct" short-lived nuclides, such as ^{41}K–^{41}Ca, ^{60}Fe–^{60}Ni, ^{53}Mn–^{53}Cr, ^{146}Sm–^{142}Nd, etc.

The isochron equation can also be graphically solved if, in the same sample, several fractions having different parent/daughter ratios ($^{27}\text{Al}/^{24}\text{Mg}$) can be analysed. In this case, and if the system remained closed after its formation, the daughter isotopic ratios plot on a line (isochron) as function of the parent/daughter elemental ratios. The slope ($^{26}\text{Al}/^{27}\text{Al})_0$ and the zero-intercept give the isotopic composition of the parent and of the daughter elements, respectively, at the time the sample was formed. Since the considered parent isotope is a short-period radioactive nuclide, its isotopic composition rapidly changes with time. The $^{26}\text{Al}/^{27}\text{Al}$ ratio decreases, for instance, by a factor of 2 in 0.7 Ma. Thus, two samples 1 and 2 formed in the same original reservoir at different times will show a formation age difference $\Delta t = t_1 - t_2$, which can be written as function of the isotopic ratios of the parent nuclides according to, in the case of ^{26}Al for instance:

$$\frac{(^{26}\text{Al}/^{27}\text{Al})_{t_1}}{(^{26}\text{Al}/^{27}\text{Al})_{t_2}} = e^{-\lambda \cdot \Delta t}.$$

2.2.3. THE LIMITS OF THE METHOD

In theory, variations in short-lived radioactive nuclides isotopic compositions should allow time differences between several samples formed from the same reservoir to be measured with a good precision (<1 Myr). Nevertheless, relative chronologies should be anchored with absolute ages derived from long-lived radioactivities. This condition is difficult to meet and remains a major limitation. Ongoing efforts to calibrate the ^{26}Al chronology of calcium, aluminium-rich inclusions (CAIs) of primitive meteorites, the oldest solar

system condensates against the U/Pb age are very promising (U/Pb age of 4567.2 ± 0.6 Ga; see discussion and references in Section 3.2.2.2).

Other limitations exist in using radioactive isotopes to date rocks. The system to be dated is assumed to have formed very quickly and to have subsequently remained closed to exchanges with gases, fluid phases, and adjacent minerals for both the parent and daughter isotopes. For shocked meteorites, this condition is usually not met and perturbations of the isotopic systems are often clearly visible. In addition, minerals do not cool instantaneously, simply because of the thermal inertia of the host planetary body. Most meteorite dates therefore reflect a cooling age, i.e., the time at which the host rock in the parent planetesimal cooled down below the so-called blocking temperature. This temperature marks the point when solid state diffusion becomes too slow to allow a redistribution of the parent and daughter isotopes. Cooling rates are not an issue for CAIs and chondrules that rapidly cooled in the nebular gas. However, the chondrite parent bodies kept accreting long after the formation of the CAIs and chondrules they host, and a protracted thermal history of the parent planetesimals heated by the decay of ^{26}Al and ^{60}Fe is expected.

Dating minerals and rocks in meteorites therefore entails more than producing isotopic "ages". It requires a deep understanding of what these ages mean with respect to the processes that lead to the isolation of the chronometers, the cooling history of their carrier, and any perturbation invalidating the basic dating premises.

Additional material about the principles of isotopic rock dating can be found in Albarède, 2001, 2003; Allègre, 2005; Faure, 1986; Vidal, 1998.

2.3. Chemistry: The Impossible use of Chemical Clocks in a Prebiotic Scope

LAURENT BOITEAU

The use of chemistry as a clock ("chemical chronology") basically relies on the quantification of molecular compounds involved in known chemical reactions (either as reactants or as products). Although in most astrophysical contexts the term "chemistry" strictly refers to element/isotope quantification, we shall not deal with these latter items since they are rather relevant to nucleosynthesis and/or radioactivity (nuclear physics). This also excludes the quantification of given chemical elements as time markers in e.g. geological stratigraphy, since the dating is not provided by chemistry itself, but rather by other physical methods. The most popular example is the anomalously high abundance of iridium and other siderophilic elements in the K/T layer, mostly considered to be directly connected to the fall of an asteroid ca. 65 Myr ago.

A preliminary requisite for using chemistry as a clock is a concern of analytical chemistry. Indeed it is necessary to be able to quantify – both accurately and precisely – the targeted molecular compound(s) from its – usually solid – matrix. Considering we have to deal with ''natural'' samples (geological or archaeological), such a problem is far from trivial: targeted organic analytes are likely to be present at trace level, in mixture with many other compounds (either similar or different), often included in a mineralized matrix, which complicates the extraction and analysis process (for a review of the complexity of this issue see Vandenabeele et al., 2005).

However it would be misleading to consider ''chemical chronology'' as just a concern of analytical chemistry, although far from negligible. The most fundamental element is chemical kinetics. In theory any set of chemical reactions could be considered, provided that the following elements are known:

- The set of reactions involving the given analyte (including catalytic processes);
- The kinetic law of these reactions;
- The boundary conditions: amount of reactants and products at time $t = 0$, as well as temperature, pressure etc.

It must be mentioned in addition that conversely to radioisotope decay (which is strictly first-order) the kinetics of most chemical reactions are dependent on pressure and – especially – on temperature (a temperature increase of 10 °C often involves a doubling of the reaction rate and probably much more for many slow reactions that may be useful for dating, see Wolfenden et al., 1999). Therefore, when these parameters are not constant the knowledge of their historicity is also necessary. An implicit condition is that the system is closed (no exchange of matter with the surrounding environment), otherwise the historicity of input/output of reactants/products must also be known. With the knowledge of the above elements, the building of a kinetic model (predicting the time-dependence of involved compounds) for given boundary conditions is possible through (numerically) solving a set of differential equations. In many cases the inverse problem can also be solved, i.e. retrieving the set of kinetic equations from monitoring the involved analytes, mostly through numerical simulations and fitting with experimental data.

In most cases however – especially in a geological/archaeological context – the problem is too open, with lack of information for instance about the historicity of temperature or the boundary conditions. Moreover, in many cases a given set of (analyte) measured values can correspond to several possible sets of boundary conditions, especially when reactions other than first-order are involved. Thus practically almost only *first-order* reactions can efficiently serve as clocks, what mostly means *unimolecular* reactions, for instance degradation of macromolecules or epimerisation of asymmetric centres.

2.3.1. SOME CHEMICAL CLOCKS AND THEIR LIMITS

2.3.1.1. *Temperature dependence*
While the variations of pressure have usually a slow influence on reaction kinetics in condensed phase (unless reaching very high values), temperature variations strongly affect chemical kinetics (according to Arrhenius' or Eyring's laws). Since the historicity of temperature is mostly unknown over geological timescales, it must be assumed to be constant, a condition very rarely fulfilled over long extents of time. This is a major drawback against the use of chemical reactions as geochronometers. Conversely however, measurement of the extent of given chemical degradations for otherwise well-dated samples can provide useful information on temperature historicity (Schroeder and Bada, 1976).

2.3.1.2. *Epimerisation of amino acids*
An example is given with the most documented reaction so far in this field, namely acid epimerisation through diagenesis of remains of dead organisms (Schoeder and Bada, 1976; Section 8.1 in Geyh and Schleicher, 1990). The validity range of such a method (on the condition of additional information on temperature historicity) has been estimated to be of the order of 10^6 yrs. Moreover, the use of this reaction as a clock entirely relies on the homo-chirality of protein residues in alive organic matter, thus being probably useless in a prebiotic context where the boundary conditions (initial enantiomeric excess) are unknown.

2.3.1.3. *Hydration of obsidian and silicate glass*
The adsorption of water at the surface of glass induces a diffusion-controlled hydration reaction, resulting into the slow growth of a hydrated layer. Due to the compactness of the glass material, the reaction front can remain very sharp over ages, being detectable through quite simple optical observations. Modelling of glass hydration kinetics allowed to make it a reliable chronometric method for samples aged up to 10^6 yr (Section 8.6 in Geyh and Schleicher, 1990).

Other chemically-based chronometric methods are mentioned in the literature (Sections 8.2–8.3 in Geyh and Schleicher, 1990), not suitable to dates earlier than the quaternary era: the degradation of amino acids (from proteins) in fossilised shells (ca. 2×10^6 yr); the measurement of nitrogen and/or collagen content in bones (ca. 10^5 yr). In addition, so-called "molecular clocks" actually based on the comparison of protein or DNA sequences of living organisms (in order to determine their "evolutive" age), are not really relevant to chemistry, but rather to molecular biology and will thus be discussed in part 2.4.

2.3.1.4. *Stable isotope fractionation*

To a certain extent, stable isotope fractionation used as a chronological marker can be relevant to chemistry, since in many cases the fractionation is the consequence of slight differences in stability and/or reactivity of isotopomers (compounds of same molecular structure varying only by their isotope composition). However in such a case chemical factors are almost indissociable from physical factors such as specific gravity and/or vapour pressure. An example is oxygen isotopic fractionation ($^{18}O/^{16}O$) during seawater evaporation (measured through oxygen isotopic ratio deviation in Antarctic ice mantle or in sediments), used as a marker of Earth temperature historicity in tertiary/quaternary eras (Gat, 1996; Section 7.2 in Geyh and Schleicher, 1990). Another chronostratigraphic time scale covering the complete phanerozoic era (0–650 Ma) relies on isotopic ratio deviation of sulphur ($\delta^{34}S$), carbon ($\delta^{13}C$) and/or strontium ($^{87}Sr/^{86}Sr$ ratio), and on correlations between theses values, such isotope fractionation having occurred upon biochemical or geochemical processes (Section 7.3 in Geyh and Schleicher, 1990).

2.3.1.5. *Time scales extent*

Even considering that the above-mentioned limitations could be overcome, the time scales of chemical processes are far from adequate for prebiotic chemistry. For instance the epimerisation of α-hydrogenated amino acids is estimated to be complete within at most 10^9 yrs (Schroeder and Bada, 1976). Polypeptide (protein) degradation is likely to be faster, while the survivability of fossil DNA (much more stable than RNA) is of the order of 10^7 yrs under geological conditions (Paabo and Wilson, 1991). Time scales based on stable isotope fractionation do not extend beyond the phanerozoic era. Applications would thus be mostly limited to "recent" palaeontology or archaeology, while time scales concerned by prebiotic events are several orders of magnitude older.

2.3.2. CONCLUSIONS

The chemical clocks mentioned above, are far from applicable to the prebiotic scope mostly because of too-short operative time scales, and because of the lack of information on boundary and environment conditions. In spite of good expectations expressed a few decades ago, long-period chemical clocks have been quite overwhelmed by the important progress meanwhile accomplished in the sensitivity of (either stable or radioactive) isotope analysis, see part 2.2.

2.4. Biology: The Molecular Clocks

EMMANUEL DOUZERY

With the mining of eukaryotic genome sequences, it is possible to assemble various sets of homologous genes or proteins, i.e., nucleotide or amino acid sequences that share common ancestry. From aligned homologous sequences, phylogenetic, evolutionary trees are reconstructed and provide two kinds of information. First, the topology of trees depicts the sisterhood of species. For example, Fungi are phylogenetically closer to animals than they are to plants (Philippe et al., 2004). Second, the branch lengths of trees depict the amount of evolution elapsed between two nodes (i.e., bifurcations, or speciation events), or between one node and a terminal taxon. On the Figure 2.4-1, taxon F did accumulate more molecular divergence than E since both last shared a common ancestor. To estimate phylogenies from molecular characters, probabilistic approaches are commonly used. For example, the maximum likelihood criterion identifies the topology and the interconnected branches that maximize the probability of exactly retrieving the input sequences under a given model of DNA or protein evolution. Each branch of a topology is characterized by a length that is the product of two quantities: the evolutionary rate of DNA or protein along that branch, and its time duration. Provided that there is one way to know the rates, and keeping in mind that branch lengths are estimated by probabilistic methods, then divergence times of species may be deduced. In the following section, different biological chronometers – the molecular evolutionary clocks – are briefly described to illustrate how it is possible to measure evolutionary rates of genomes in order to deduce species divergence times.

2.4.1. HISTORICAL PERSPECTIVE ON THE MOLECULAR CLOCK

Forty years ago, a linear, increasing relationship between the number of amino acid differences among proteins of vertebrate species, e.g. globins, and the age of the common ancestor of these species as measured by paleontology was evidenced (Zuckerkandl and Pauling, 1965). Molecular evolutionary clocks were born. Protein and DNA clocks were unexpected, and questioned, as researchers thought that morphological and molecular evolution proceeded in the same way, i.e., with large rate variations over time and among species. However, even if each protein seemed to exhibit a constant rate through time, different proteins had different absolute rates, e.g., exceedingly slow for histones, slow for cytochrome c, intermediate for globins, and faster for fibrinopeptides (Dickerson, 1971).
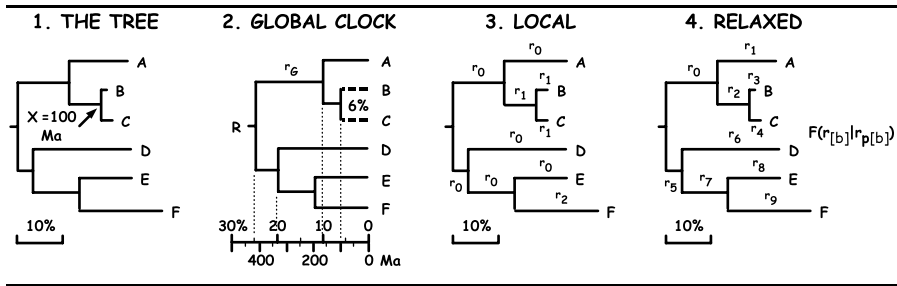
Figure 2.4-1 to −4. Phylogenetic tree reconstructed from homologous molecular sequences and depicting the evolutionary relationships among the six taxa A–F. The time line is horizontal, and branch lengths are proportional to the amount of accumulated molecular divergence. The scale is 10 nucleotide or amino acid substitutions per 100 sites compared (%). Let X be the most recent common ancestor of B and C. X is here the external fossil calibration, with a paleontological age of 100 million years (Ma). 2.- The previous tree is converted into a clocklike tree, where all taxa are equidistant from the origin of the tree (R, root). Relative rate tests evaluate the degree of distortion between the initial and clocklike trees. The maximum likelihood estimate of branch lengths XB = XC corresponds to 6% (dashed lines). The absolute substitution rate per branch is therefore $r_G = 0.06\%$/Ma. Extrapolation of this global clock allows the calculation of divergence times (see the time scale expressed in Ma). For example, RA = 25%, indicating that the age of R is $RA/r_G = 417$ Ma. 3.- The initial tree is converted into a maximum likelihood local clock tree, with three different rates: r_0, assigned to 6 branches, r_1 to three branches, and r_2 to one branch, with $r_1 < r_0 < r_2$. Knowing the local clocks $r_0 - r_2$, divergence times are calculated. 4.- Rates are allowed to vary along branches, and one distinct rate is estimated per branch. The rate of a given branch b ($r_{[b]}$) is linked to the rate of its parental branch ($r_{p[b]}$). For example, $r_{p[1]} = r_0$. In the relaxed clock approaches, the distributions of rates $r_0 - r_9$ and divergence times are estimated under $F(r_{[b]}|r_{p[b]})$, a penalty function that reduces too large rate variations between daughter and parental branches.

The neutral theory of molecular evolution provided an explanation to the quite regular ticking of the molecular chronometers (Kimura and Ohta, 1971). Mutations in genomes are either neutral (or quasi-neutral) – i.e., without effect (or nearly so) on the fitness of organisms – or under natural selection (positively or negatively selected). In natural populations, neutral substitutions accumulate at a rate that is only influenced by the mutation rate. As long as a gene contains significantly more neutral positions than selected, and as the mutation rate remains unchanged, then the evolution of DNA will be clocklike (Bromham and Penny, 2003).

The behaviour of biological chronometers, DNA and protein clocks, is a discrete, probabilistic process. In molecular evolution, a Poisson distribution is commonly used to model the time intervals between independent nucleotide or amino acid substitution events – the "ticks" of the clock. This distribution is characterized by the fact that its variance is equal to its mean, indicating that the ticks of the molecular clock are regular and random. Biological

chronometers should therefore be seen as stochastic clocks rather than perfect, deterministic metronomes. Similarly, geological chronometers based on radioactivity decay follow the same stochastic behaviours (see part 2.2).

2.4.2. THE GLOBAL MOLECULAR CLOCK: A SINGLE RATE APPROACH

A constant rate of molecular evolution over the whole phylogenetic tree will be called a *global molecular clock*. Its calibration by an external date based on taxa with a rich fossil record is used to estimate divergence times for other living organisms (Figure 2.4-2). However, with the growing number of studies using the molecular clock to estimate the divergence age of organisms, different and independent problems appeared (Graur and Martin, 2004).

A first, important issue of the molecular clock approach is the fact that a global clocklike behaviour of the sequences is certainly not the rule. Several empirical studies evidenced variations in the rate of molecular evolution among taxa, both at the nucleotide and amino acid levels. These trends are not restricted to a few genes and proteins. For example, a sample of 129 proteins from an animal like a drosophila and a plant like the rice accumulated the same amount of differences, whereas trypanosomes (flagellate parasites) evolve at least twice faster than humans with respect to the amino acid replacement rate through time (Philippe et al., 2004). Statistical tests were therefore developed to measure the degree of departure of sequence data from the clock hypothesis. The most famous one is the relative rate test (Sarich and Wilson, 1973). Let AB and AC be the genetic distances from the two compared species (B and C) relative to a third, external one (A: Figure 2.4–1). If AB and AC are nearly equal, then the evolution of B and C is considered as clocklike. Now, if we consider the external species D relative to E and F, then DF > DE, and F is considered to evolve faster than E: their evolution is not clocklike. An other test is built in a maximum likelihood framework. The significance of the loss of likelihood between a clocklike set of branch lengths relative to the one of the same set of branches without the global clock assumption is compared by a likelihood ratio test (Felsenstein, 1988). However, these tests display a low resolving power, even if this may be partially corrected through the increase of the number of species and nucleotide or amino acid sites analysed (Philippe et al., 1994; Bromham et al., 2000; Robinson-Rechavi and Huchon, 2000). Though questionable when rate variation is the rule rather than the exception, the systematic elimination of erratic molecular rates across taxa and/or genes has been proposed, in order to restrict molecular dating analyses to the more clocklike data sets (Ayala et al., 1998; Kumar and Hedges, 1998). For example, the use of 39 constant rate proteins and the paleontological reference of a mammals/

birds split at 310 ± 0 Ma was extrapolated to estimate that the animals/fungi split may have occurred $1{,}532 \pm 75$ Ma ago (Wang et al., 1999).

Interestingly, multiple substitutions on the same DNA or protein position across the taxa compared can yield a saturation phenomenon, leading to observe a virtually similar amount of genetic divergence among the sequences compared. When the noisiest sites are discarded, changes in the topology of the phylogenetic tree and in the evolutionary rates may be revealed (Brinkmann and Philippe, 1999; Burleigh and Mathews, 2004): sequences initially thought to evolve clocklike actually display differences of substitution rates.

A second problem of the global clock approach is the use of a unique calibration point. As a fixed time point, it will ignore the inherent uncertainty of the fossil record. Moreover, when the calibration is chosen within a slow-evolving lineage (or conversely, in a fast-evolving lineage), the inferred rate of substitution will overestimate (or conversely, underestimate) the true divergence times. Actually, to explain the length of a given branch, e.g. 10% of DNA substitutions, a faster rate of evolution (e.g., 1%/Ma) will involve a shorter time duration (10 Ma), whereas a slower rate (0.1%/Ma) will involve a longer time (100 Ma). In numerous recent studies, vertebrates have been taken as the single calibrating fossils (e.g., Wang et al., 1999). However, vertebrates apparently display a slow rate of genomic evolution, at least for the proteins usually sampled (Philippe et al., 2005). There is therefore a concern that the deep divergence times observed between the major eukaryotic kingdoms, e.g., animals or fungi, would reflect the use of a single paleontological reference to calibrate the slow-evolving vertebrates (Douzery et al., 2004). To circumvent the above-mentioned problems, alternative molecular clock approaches have been designed which are based on the estimate of a few or several rates rather than a single one.

2.4.3. THE LOCAL MOLECULAR CLOCKS: A FEW RATE APPROACH

When a phylogeny is reconstructed under maximum likelihood, two extreme models of substitution rates among branches may be used. The first assumes one independent rate for each branch (Figure 2.4-1). The second assumes a single rate for all branches, a situation called the global molecular clock (see above). An intermediate approach has been suggested: the *local molecular clock model* assumes that some branches are characterized by a first rate–for example those connecting the most closely related species–whereas other branches display a second, distinct rate (Rambaut and Bromham, 1998; Yoder and Yang, 2000). In other words, local constancy of rates is tolerated despite potential greater variation at larger phylogenetic scales in the tree (Figure 2.4-3). Application of the local clocks to empirical data suggests that this approach is a reasonable compromise between too few and too much

evolutionary rate classes per phylogenetic tree (Douzery et al., 2003). However, a subsequent difficulty is to identify the set of branches which will share the same rate, as well as the number of rate classes to assign on the whole tree.

Recent progresses in the local clock framework involve (i) the possibility to deal with multiple genes and multiple calibration points (Yang and Yoder, 2003), and (ii) the development of an improved algorithm – combining likelihood, Bayesian, and rate-smoothing procedures – to automatically assign branches to rate groups during local molecular clocks analyses (Yang, 2004).

2.4.4. THE RELAXED MOLECULAR CLOCKS: A MULTIPLE RATE APPROACH

As a solution to circumvent the confounding effect of non-clocklike behaviour of mutations, dating methods have been developed to relax the molecular clock assumption by allowing discrete or continuous variations of the rate of molecular evolution along branches of a phylogenetic tree (Sanderson, 1997, 2002; Thorne et al., 1998; Huelsenbeck et al., 2000; Kishino et al., 2001; Thorne and Kishino, 2002; Aris-Brosou and Yang, 2002, 2003). Changes in the rate from a parental branch to a daughter branch are governed by a penalty function (Welch and Bromham, 2005), which reduces too large variations (Figure 2.4-4). Penalties are either simple expressions, like the quadratic one – $(r_{[b]}-r_{p[b]})^2$ – which is time independent (Sanderson, 1997, 2002), or more complex functions which depend upon time (stationary lognormal: Kishino et al., 2001; exponential: Aris-Brosou and Yang, 2002).

Some of these approaches are implemented in a Bayesian framework, with estimation of the distributions of rates and divergence times, recapitulated as values with associated uncertainty (credibility) intervals. Moreover, the uncertainty of paleontological estimates is explicitly incorporated in the form of prior constraints on divergence times provided by fossil information (Kishino et al., 2001). Calibration time intervals for several independent nodes in the tree may as well be used simultaneously to reduce the impact of choosing a particular calibration reference. This method has been convincingly applied to understand the chronological evolution of very diverse taxonomic groups, like viruses (Korber et al., 2000), plants (Bell et al., 2005), mammals (Springer et al., 2003), and eukaryotes (Douzery et al., 2004). In the latter study, the relaxed clock on 129 proteins is calibrated by six fossil references, and suggests that the animals/fungi split may have occurred 984 ± 65 Ma ago. This estimate, markedly smaller than the $1,532 \pm 75$ Ma of Wang et al. (1999), is likely to be more accurate, owing to the use of a flexible molecular clock, and a greater number of proteins, species, and

calibrations. It also illustrates how different data, calibrations and methods can provide contrasted timeline estimates.

2.4.5. THE FUTURE MOLECULAR CLOCKS: ACCURACY AND PRECISION

During the past four decades, molecular clocks have became an invaluable tool for reconstructing evolutionary timescales, opening new views on our understanding of the temporal origin and diversification of species (Kumar, 2005). However, to facilitate in the near future the comparison between rocks and clocks, critical paleontological references should be developed (Müller and Reisz, 2005), and molecular dating should become more accurate and more precise. Enhanced accuracy of molecular clocks might be achieved through the analysis of more genes for more species, but also through the development of realistic models of rate change, with discrete as well as continuous variations of evolutionary rate through time (Ho et al., 2005). Greater precision is however not warranted due to the inherent, stochastic nature of biological chronometers.

2.5. The Triple Clock of Life in the Solar System

THIERRY MONTMERLE AND MURIEL GARGAUD

2.5.1. IS THERE A BEGINING? THE PROBLEM OF "TIME ZERO" AND THE LOGARITHMIC CLOCK

As discussed in Chapter 1, the solar system must *a priori* have a "beginning". In other words, there must exist a "time zero" $t_0{}^*$ to mark the origin of the solar system, so that by definition the Sun is formed at $t = t_0{}^*$, and then everything proceeds and can be dated according to a regular time scale: the formation of the Sun, disk evolution, condensation of the first solids, planet formation, existence of oceans, emergence of life, etc...But as a matter of fact, for very fundamental reasons similar to those of the universe itself, to define $t_0{}^*$ as the age of the solar system is astrophysically impossible. Indeed, even if the universe is expanding, and a protostar is contracting, the structure of the equations that govern these evolutions is such that time flows *logarithmically*, not linearly. In other words, looking for $t_0{}^*$ is like going backwards in time in units of fractions of an arbitrary reference time, t_r, say: $t_r/10$, $t_r/100$, $t_r/1000$, etc. As for Zenon's paradox, the ultimate origin, $t_0{}^*$, can never be reached, only approximated to a predefined level. At least as long as the equations remain valid: in the case of star formation, for instance, it is clear that,

starting from a uniform medium in gravitational equilibrium (which is essentially the state of molecular clouds), stars should never form. So some external disturbance, not present in the equations, has to trigger the gravitational collapse (see section 3.1.1). Then this "initial" disturbance is forgotten very fast, and the "astronomical", logarithmic clock starts ticking: time just flows, and only relative times (time scales, or time intervals), corresponding to successive phases dominated by specific physical mechanisms, are meaningful.

We have illustrated this for the solar system in Figure 2.5.1. The first stage of the formation of the Sun is free-fall gravitational collapse of a molecular core, which, for solar-type stars, takes about 10^4 yrs. The protosun is thus essentially a rapidly evolving dense and extended envelope, but since this envelope is made of dust grains and gas with heavy elements, at some point it becomes opaque to its own radiation. Then the gravitational energy becomes trapped: a slower evolution ensues, regulated by radiative transfer (cooling) of its outer layers. The next timescale for evolution is about 10^5 yrs, when the formation of the Sun is eventually completed (Chapter 3.1). Indeed, at the centre, a dense protosolar embryo has formed, and here also the evolution is
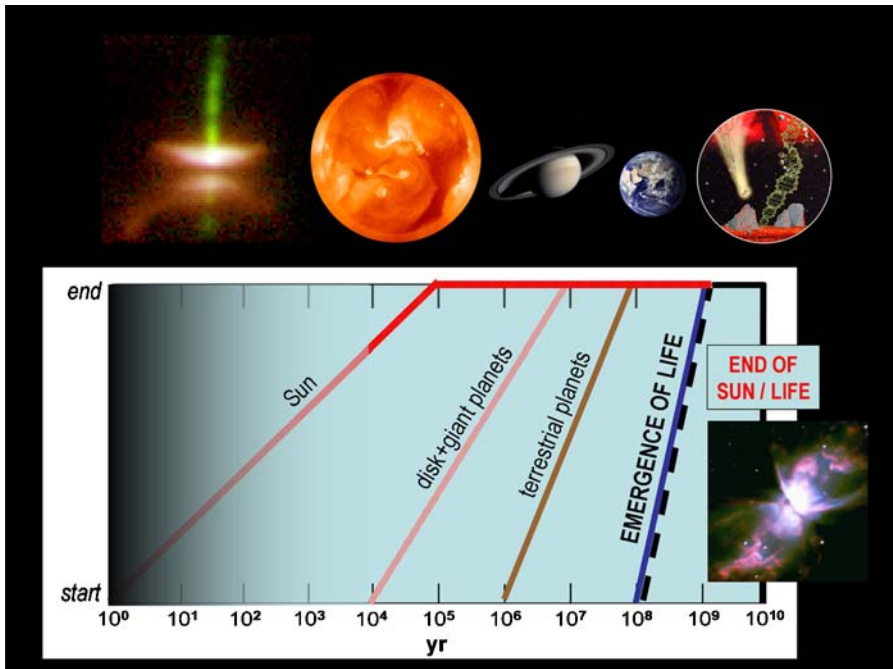

Figure 2.5.1. A very simplified "astronomical history" of the solar system, using a logarithmic clock, from the time of the formation of the Sun as a protostar, until its end as a planetary nebula. The detailed history is the subject of Chapter 3.

regulated by the opacity, but inside a much denser and hotter body. A quasi-static gravitational equilibrium becomes established, which will last until nuclear reactions start 10^8 yrs later when the Sun reaches the main sequence. Meanwhile, and because of rotation, a circumstellar accretion disk forms. This disk has its own evolution, and the growth of dust grains under the influence of dynamical interactions has a characteristic timescale of 10^6 yrs. Then planetesimals collide and eventually build giant planets on timescales of 10^7 yrs. (Chapter 3.2). Finally, terrestrial planets form in 10^8 yrs (Chapter 3.3), which, by coincidence in the case of the solar system, is also the time-scale for the Sun to arrive on the main sequence.

This global (albeit very simplified) chronology of the so-called ''pre-main sequence'' phases of evolution of (solar-like) stars is also apparent in the ''Herzsprung–Russell Diagram'' introduced in Section 2.1 (except for the earliest stages which, being embedded and going through optically invisible phases, cannot be plotted on such a diagram). So even though t_0^* cannot be defined strictly speaking, the succession of phases, with its clock scaled (in yrs) in powers of 10, is well-defined.

The history of the solar system can be continued using the same clock. On this scale, life emerges in 10^9 yrs but must end at 10^{10} yrs because of the evolution of the Sun, which will become a red giant and engulf the whole solar system before becoming a planetary nebula (Section 2.1). These are the two only important events of the solar system at this stage! (Note that the characteristic timescale of 10^{10} yrs is also valid for stars of mass < 0.7 $M_\odot$, which live longer than the age of the universe, itself of the order of 10^{10} yrs.)

As Figure 2.5.1 illustrates, the ''powers of 10'' stages described above also have a certain duration, and at a given time some stages end while others have begun: for instance, circumstellar disks already exist at the protostellar stage (Section 3.2.1), and similarly the embryos of terrestrial planets (Section 3.2.4 and 3.3.1) are already present in the course of disk evolution. Strictly speaking, the ''start'' point of each phase is as impossible to define as t_0^* itself, since phase n already includes some evolution of phase $n + 1$. Figure 2.5.1 is only meant to give schematically a very synthetic idea of the astronomical chronology described in Chapter 3. What is certainly noteworthy, however, is that since the existence of the Earth is a prerequisite for the emergence of life as we know it, the slope (rate of growth) appears much steeper for life as it is for all the previous phases: paradoxically (in this chronology) life develops much faster that the Sun itself! And certainly the emergence of life is short (10%) compared with the lifetime of the Sun. We will come back to some important consequences of this fact in the next paragraph.
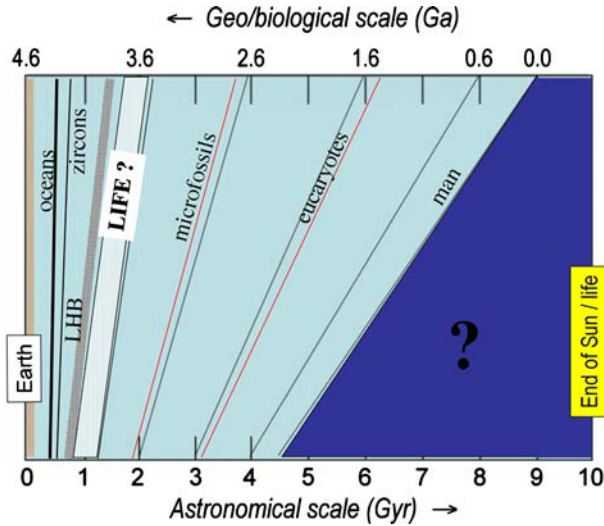
Figure 2.5.2. The astronomical, biological and geological histories of the solar system, using linear clocks. While time proceeds *forward* in astronomy (conventional unit: Gyr) since the formation of the Sun and planets (which are very short compared with the lifetime of the Sun, hence look almost instantaneous), time is measured *backwards* from 1950 AD (the "Present") in geology and biology (conventional unit: Ga). The main geological and biological events of these histories, as described in the text, are indicated in both scales.

2.5.2. ASTRONOMY VS. GEOLOGICAL AND BIOLOGICAL CHRONOLOGIES: THE LINEAR CLOCKS

Once the Earth is formed, we become interested in the chronology of events that have shaped its evolution, with the ultimate goal of understanding how life emerged, and its subsequent evolution into organized, self-replicating and increasingly complex structures. The essence of dating events comes from geology, and it is clear that the numbers obtained by all methods (radioactive decay, geological layers, etc.) are linearly ordered. In other words, to describe the corresponding chronology we have to adopt a perhaps more familiar *linear* clock. This necessary switch from the previous clock offers a paradox quite similar to that mentioned previously about life: as illustrated in Figure 2.5.2, on a linear astronomical scale, the Sun and the Earth are formed essentially instantaneously (1% of the lifetime of the Sun).

The "linear clock" can then be used in two different ways. Because when using this clock the formation of the Sun and of the Earth are almost simultaneous, the exact definition of t_0* is not important: it does not really matter to know whether the age of the oldest meteorites is 4.567 Gyr or even 3 Gyr – what is important is that this age is much larger than the duration of the formation of the Sun and terrestrial planets. However the astronomical

scale is graduated with *increasing* values of time, which is the natural way to follow the evolution of the Sun (for instance, small, but possibly important fluctuations in its luminosity can be observed) and incorporate the *future of the Earth*, at least, again, until its doom as a vaporized planet *inside* the red giant Sun, within 5.5 Gyr. (We are already half-way into this evolution, of which the last steps will take a few million years, so here also will look on this scale as brief as the formation of the Sun.)

Correspondingly, geologists, who are the watchmakers of biologists, naturally measure the time going *backwards*. Their clock is still linear, but is graduated starting from 1950 AD: the ''Present'' (see Chapter 1 and Section 2.2). So while for solar system studies the astronomical time flows forward,[3] by necessity geologists have to look backwards so are concerned only with the past, not the future, of the Earth. (Note also that on all scales the emergence of man is instantaneous.)

The correspondence between the linear astronomical and ''geobiological'' clocks is illustrated in Figure 2.5.2, covering all known periods of the past (geology and biology) and of the future (astronomy). Also shown are the main events that occurred in the remote history of the Earth, as described in detail in the following chapters, from the formation of the first oceans, the so-called Late Heavy Bombardment (LHB), to the appearance of eukaryotes, bracketing the still controversial period where life is thought to have appeared. A summary of the main geological, chemical and biological events covering this period is presented in Chapters 8 and 9.

References

Albarède, F.: 2001, *La géochimie*, Paris, 190 pp.
Albarède, F.: 2003. *Geochemistry: An Introduction*, Cambridge University Press, Cambridge, 262 pp.
Allègre, C. J.: 2005. *Géologie Isotopique*, Belin, Paris, 495 pp.

---

[3] Note that this is not true in cosmology, where astronomers can explore the past of the universe, since the more distant a galaxy (say) is, the younger it looks to us because of the finite time light takes to travel.

Aris-Brosou, S. and Yang, Z.: 2002, *Syst. Biol.* **51**, 703–714.

Aris-Brosou, S. and Yang, Z.: 2003, *Mol. Biol. Evol.* **20**, 1947–1954.

Ayala, F. J., Rzhetsky, A. and Ayala, F. J.: 1998, *Proc. Natl. Acad. Sci. USA* **95**, 606–611.

Bell, C. D., Soltis, D. E. and Soltis, P. S.: 2005, *Evolution* **59**, 1245–1258.

Brinkmann, H. and Philippe, H.: 1999, *Mol. Biol. Evol.* **16**, 817–825.

Bromham, L. and Penny, D.: 2003, *Nature Rev. Genet.* **4**, 216–224.

Bromham, L., Penny, D., Rambaut, A. and Hendy, M. D.: 2000, *J. Mol. Evol.* **50**, 296–301.

Burleigh, J. G. and Mathews, S.: 2004, *Am. J. Bot.* **91**, 1599–1613.

Chabrier, G. and Baraffe, I.: 2000, *Ann. Rev. Astr. Ap.* **38**, 337–377.

Dickerson, R. E.: 1971, *J. Mol. Evol.* **1**, 26–45.

Douzery, E. J. P., Delsuc, F., Stanhope, M. J. and Huchon, D.: 2003, *J. Mol. Evol.* **57**, S201–S213.

Douzery, E. J. P., Snell, E. A., Bapteste, E., Delsuc, F. and Philippe, H.: 2004, *Proc Natl. Acad. Sci. USA* **101**, 15386–15391.

Faure, G.: 1986. *Principles of Isotope Geology*, John Wiley and sons, New York, 589 pp.

Felsenstein, J.: 1988, *Ann. Rev. Genet.* **22**, 521–565.

Gat, J. R.: 1996, *Annu. Rev. Earth Planet. Sci.* **24**, 225–262.

Geyh, M. A. and Schleicher, H.: 1990, in *Absolute Age Determination*, Springer-Verlag, Berlin, 503 pp.

Graur, D. and Martin, W.: 2004, *Trends Genet.* **20**, 80–86.

Hayashi, C.: 1966, *Ann. Rev. Astron. Astrophys.* **4**, 171–192.

Hillenbrand, L. A.: 1997, *Astron. J.* **113**, 1733–1768.

Ho, S. Y. W., Phillips, M. J., Drummond, A. J. and Cooper, A.: 2005, *Mol. Biol. Evol.* **22**, 1355–1363.

Huelsenbeck, J. P., Larget, B. and Swofford, D.: 2000, *Genetics* **154**, 1879–1892.

Kimura, M. and Ohta, T.: 1971, *J. Mol. Evol.* **1**, 1–17.

Kishino, H., Thorne, J. L. and Bruno, W. J.: 2001, *Mol. Biol. Evol.* **18**, 352–361.

Korber, B., Muldoon, M., Theiler, J., Gao, F., Gupta, R., Lapedes, A., Hahn, B. H., Wolinsky, S. and Bhattacharya, T.: 2000, *Science* **288**, 1789–1796.

Kumar, S.: 2005, *Nature Rev. Genet.* **6**, 654–662.

Kumar, S. and Hedges, S. B.: 1998, *Nature* **392**, 917–920.

Montmerle, T. and Prantzos, N.: 1988, *Soleils Eclatés*, Presses du CNRS/CEA, 160 pp.

Müller, J. and Reisz, R. R.: 2005, *BioEssays* **27**, 1069–1075.

Paabo, S. and Wilson, A.: 1991, *Curr. Biol.* **1**, 45–46.

Palla, F. and Stahler, S. W.: 2001, *Astrophys. J.* **553**, 299–306.

Philippe, H., Lartillot, N. and Brinkmann, H.: 2005, *Mol. Biol. Evol.* **22**, 1246–1253.

Philippe, H., Snell, E. A., Bapteste, E., Lopez, P., Holland, P. W. H. and Casane, D.: 2004, *Mol. Biol. Evol.* **9**, 1740–1752.

Philippe, H., Sörhannus, U., Baroin, A., Perasso, R., Gasse, F. and Adoutte, A.: 1994, *J. Evol. Biol.* **7**, 247–265.

Rambaut, A. and Bromham, L.: 1998, *Mol. Biol. Evol.* **15**, 442–448.

Robinson-Rechavi, M. and Huchon, D.: 2000, *Bioinformatics* **16**, 296–297.

Sanderson, M. J.: 1997, *Mol. Biol. Evol.* **14**, 1218–1231.

Sanderson, M. J.: 2002, *Mol. Biol. Evol.* **19**, 101–109.

Sarich, V. M. and Wilson, A. C.: 1973, *Science* **179**, 1144–1147.

Schroeder, R. A. and Bada, J. L.: 1976, *Earth Sci. Rev.* **12**, 347–391.

Springer, M. S., Murphy, W. J., Eizirik, E. and O'Brien, S. J.: 2003, *Proc. Natl. Acad. Sci. USA* **100**, 1056–1061.

Thorne, J. L. and Kishino, H.: 2002, *Syst. Biol.* **51**, 689–702.

Thorne, J. L., Kishino, H. and Painter, I. S.: 1998, *Mol. Biol. Evol.* **15**, 1647–1657.

Vandenabeele-Trambouze, O., Garrelly, L. and Dobrijevic, M.: 2005, in M. Gargaud, P. Claeys and H. Martin (eds.), *Des atomes aux planètes habitables*, Presses Universitaires de Bordeaux, Bordeaux, pp. 323–356.

Vidal, P.: 1998. *Géochimie*, Dunod, Paris, 190 pp.

Wang, D. Y., Kumar, S. and Hedges, S. B.: 1999, *Proc. R. Soc. Lond. B, Biol. Sci.* **266**, 163–171.

Welch, J. J. and Bromham, L.: 2005, *Trends Ecol. Evol.* **20,** 320–327.

Wolfenden, R., Snider, M., Ridgway, C. and Miller, B.: 1999, *J. Am. Chem. Soc.* **121**, 7419–7420.

Yang, Z.: 2004, *Act. Zool. Sin.* **50**, 645–656.

Yang, Z. H. and Yoder, A. D.: 2003, *Syst. Biol.* **52**, 705–716.

Yoder, A. D. and Yang, Z.: 2000, *Mol. Biol. Evol.* **17**, 1081–1190.

Zuckerkandl, E. and Pauling, L.: 1965, in V. Bryson and H. J. Vogel (eds.), *Evolving Genes and Proteins*, Academic Press, New York, pp. 97–166.